Research Article | Vol. 9, No. 2 | 1 Feb 2018 | BIOMEDICAL OPTICS EXPRESS 771

Biomedical Optics EXPRESS

Optical tweezers system for live stem cell organization at the single-cell level

PEIFENG JING,[1] YANNAN LIU,[1] ETHAN G. KEELER,[1] NELLY M. CRUZ,[2] BENJAMIN S. FREEDMAN,[2] AND LIH Y. LIN[1]

[1]*Department of Electrical Engineering, University of Washington, 185 Stevens Way, Seattle, WA 98195, USA*

[2]*Division of Nephrology, Kidney Research Institute, and Institute for Stem Cell and Regenerative Medicine, Department of Medicine, University of Washington School of Medicine, 850 Republican St., Seattle, WA 98109, USA*

**lylin@uw.edu*

Abstract: Cell manipulation is one of the most impactful applications for optical tweezers, and derived from this promise, we demonstrate a new optical tweezers system for the study of cell adhesion and organization. This method utilizes photonic-crystal-enhanced optical tweezers to manipulate cells with low laser intensities. By doing so, it enables effective cell patterning and culturing within the conditions necessary for successful differentiation and colony formation of human pluripotent stem cells. To this end, the biocompatibility of plasma-treated parylene-C for cell culturing was studied, and a thorough characterization of cellular interactive forces was performed using this system. Furthermore, this study also demonstrates construction of patterned cell arrays at arbitrary positions with micrometer-scale precision.

OCIS codes: (350.4855) Optical tweezers or optical manipulation; (170.1420) Biology.

References and links

1. A. Warmflash, B. Sorre, F. Etoc, E. D. Siggia, and A. H. Brivanlou, "A method to recapitulate early embryonic spatial patterning in human embryonic stem cells," Nat. Methods **11**(8), 847–854 (2014).
2. Z. Ma, J. Wang, P. Loskill, N. Huebsch, S. Koo, F. L. Svedlund, N. C. Marks, E. W. Hua, C. P. Grigoropoulos, B. R. Conklin, and K. E. Healy, "Self-organizing human cardiac microchambers mediated by geometric confinement," Nat. Commun. **6**, 7413 (2015).
3. W. Reeves, J. P. Caulfield, and M. G. Farquhar, "Differentiation of epithelial foot processes and filtration slits: sequential appearance of occluding junctions, epithelial polyanion, and slit membranes in developing glomeruli," Lab. Invest. **39**(2), 90–100 (1978).
4. B. Hartleben, H. Schweizer, P. Lübben, M. P. Bartram, C. C. Möller, R. Herr, C. Wei, E. Neumann-Haefelin, B. Schermer, H. Zentgraf, D. Kerjaschki, J. Reiser, G. Walz, T. Benzing, and T. B. Huber, "Neph-Nephrin proteins bind the Par3-Par6-atypical protein kinase C (aPKC) complex to regulate podocyte cell polarity," J. Biol. Chem. **283**(34), 23033–23038 (2008).
5. J. Reiser, W. Kriz, M. Kretzler, and P. Mundel, "The glomerular slit diaphragm is a modified adherens junction," J. Am. Soc. Nephrol. **11**(1), 1–8 (2000).
6. Y. K. Kim, I. Refaeli, C. R. Brooks, P. Jing, R. E. Gulieva, M. R. Hughes, N. M. Cruz, Y. Liu, A. J. Churchill, Y. Wang, H. Fu, J. W. Pippin, L. Y. Lin, S. J. Shankland, A. W. Vogl, K. M. McNagny, and B. S. Freedman, *Gene-Edited Human Kidney Organoids Reveal Mechanisms of Disease in Podocyte Development.* Stem Cells, 2017. **35**(12): p. 2366–2378.
7. M. Prass, K. Jacobson, A. Mogilner, and M. Radmacher, "Direct measurement of the lamellipodial protrusive force in a migrating cell," J. Cell Biol. **174**(6), 767–772 (2006).
8. C. Gosse and V. Croquette, "Magnetic tweezers: micromanipulation and force measurement at the molecular level," Biophys. J. **82**(6), 3314–3329 (2002).
9. M. Eastwood, D. A. McGrouther, and R. A. Brown, "A culture force monitor for measurement of contraction forces generated in human dermal fibroblast cultures: evidence for cell-matrix mechanical signalling," Biochim. Biophys. Acta **1201**(2), 186–192 (1994).
10. J. Helenius, C. P. Heisenberg, H. E. Gaub, and D. J. Muller, "Single-cell force spectroscopy," J. Cell Sci. **121**(11), 1785–1791 (2008).
11. P. H. Puech, K. Poole, D. Knebel, and D. J. Muller, "A new technical approach to quantify cell-cell adhesion forces by AFM," Ultramicroscopy **106**(8-9), 637–644 (2006).

#315644 https://doi.org/10.1364/BOE.9.000771
Journal © 2018 Received 14 Dec 2017; revised 17 Jan 2018; accepted 18 Jan 2018; published 25 Jan 2018

Biomedical Optics EXPRESS

12. R. I. Litvinov, H. Shuman, J. S. Bennett, and J. W. Weisel, "Binding strength and activation state of single fibrinogen-integrin pairs on living cells," Proc. Natl. Acad. Sci. U.S.A. **99**(11), 7426–7431 (2002).
13. O. Thoumine, P. Kocian, A. Kottelat, and J. J. Meister, "Short-term binding of fibroblasts to fibronectin: optical tweezers experiments and probabilistic analysis," Eur. Biophys. J. **29**(6), 398–408 (2000).
14. E. Evans, K. Ritchie, and R. Merkel, "Sensitive force technique to probe molecular adhesion and structural linkages at biological interfaces," Biophys. J. **68**(6), 2580–2587 (1995).
15. N. Q. Balaban, U. S. Schwarz, D. Riveline, P. Goichberg, G. Tzur, I. Sabanay, D. Mahalu, S. Safran, A. Bershadsky, L. Addadi, and B. Geiger, "Force and focal adhesion assembly: a close relationship studied using elastic micropatterned substrates," Nat. Cell Biol. **3**(5), 466–472 (2001).
16. A. Kloboucek, A. Behrisch, J. Faix, and E. Sackmann, "Adhesion-induced receptor segregation and adhesion plaque formation: A model membrane study," Biophys. J. **77**(4), 2311–2328 (1999).
17. O. Thoumine, A. Ott, O. Cardoso, and J. J. Meister, "Microplates: a new tool for manipulation and mechanical perturbation of individual cells," J. Biochem. Biophys. Methods **39**(1-2), 47–62 (1999).
18. J. M. Atienza, J. Zhu, X. Wang, X. Xu, and Y. Abassi, "Dynamic monitoring of cell adhesion and spreading on microelectronic sensor arrays," J. Biomol. Screen. **10**(8), 795–805 (2005).
19. D. G. Grier, "A revolution in optical manipulation," Nature **424**(6950), 810–816 (2003).
20. C. Xie, C. Goodman, M. Dinno, and Y. Q. Li, "Real-time Raman spectroscopy of optically trapped living cells and organelles," Opt. Express **12**(25), 6208–6214 (2004).
21. C. Bustamante, Z. Bryant, and S. B. Smith, "Ten years of tension: single-molecule DNA mechanics," Nature **421**(6921), 423–427 (2003).
22. K. C. Neuman, E. H. Chadd, G. F. Liou, K. Bergman, and S. M. Block, "Characterization of photodamage to Escherichia coli in optical traps," Biophys. J. **77**(5), 2856–2863 (1999).
23. U. Mirsaidov, W. Timp, K. Timp, M. Mir, P. Matsudaira, and G. Timp, "Optimal optical trap for bacterial viability," Phys. Rev. E Stat. Nonlin. Soft Matter Phys. **78**(2 Pt 1), 021910 (2008).
24. P. Y. Chiou, A. T. Ohta, and M. C. Wu, "Massively parallel manipulation of single cells and microparticles using optical images," Nature **436**(7049), 370–372 (2005).
25. M. L. Juan, M. Righini, and R. Quidant, "Plasmon nano-optical tweezers," Nat. Photonics **5**(6), 349–356 (2011).
26. P. F. Jing, J. D. Wu, and L. Y. Lin, "Patterned Optical Trapping with Two-Dimensional Photonic Crystals," ACS Photonics **1**(5), 398–402 (2014).
27. P. Jing, J. Wu, G. W. Liu, E. G. Keeler, S. H. Pun, and L. Y. Lin, "Photonic Crystal Optical Tweezers with High Efficiency for Live Biological Samples and Viability Characterization," Sci. Rep. **6**(1), 19924 (2016).
28. J. A. Thomson, J. Itskovitz-Eldor, S. S. Shapiro, M. A. Waknitz, J. J. Swiergiel, V. S. Marshall, and J. M. Jones, "Embryonic stem cell lines derived from human blastocysts," Science **282**(5391), 1145–1147 (1998).
29. K. Takahashi, K. Tanabe, M. Ohnuki, M. Narita, T. Ichisaka, K. Tomoda, and S. Yamanaka, "Induction of pluripotent stem cells from adult human fibroblasts by defined factors," Cell **131**(5), 861–872 (2007).
30. T. Y. Chang, V. G. Yadav, S. De Leo, A. Mohedas, B. Rajalingam, C. L. Chen, S. Selvarasah, M. R. Dokmeci, and A. Khademhosseini, "Cell and protein compatibility of parylene-C surfaces," Langmuir **23**(23), 11718–11725 (2007).
31. T. A. Nieminen, V. L. Y. Loke, A. B. Stilgoe, G. Knoner, A. M. Branczyk, N. R. Heckenberg, and H. Rubinsztein-Dunlop, "Optical tweezers computational toolbox," J. Opt. A, Pure Appl. Opt. **9**(8), S196–S203 (2007).
32. P. Jing, K. Winston, Y. C. Chen, B. Freedman, and L. Y. Lin, *Patterning and Colonizing Stem Cells with Optical Trapping*, in *Optical Trapping Applications*. 2017, Optical Society of America: San Diego, USA. p. OtM4E. 2.

1. Introduction

Cellular spatial patterning and geometrical confinement are postulated as important factors in tissue development and disease [1, 2]. To study these factors, cell cultures can provide a useful model system; however, we are still limited in our ability to position cells with specific geometries in culture, particularly at the single-cell level. Accompanying this need for position control, we also have not yet developed accurate methodologies to measure and characterize the forces arising between individual cells that establish geometrical separation.

The forces between individual cells are directly applied to cellular interaction and junctional formation. For example, the foot processes of the podocytes are linked together by a specialized junction that is significant in filtering small molecules such as water and salts in the blood [3–5]. The podocalyxin proteins on the cell membrane are strongly negatively charged, and this is hypothesized to be the primary factor in junction formation [6]. There are many technologies developed to measure the attachment or adhesive forces of cells, including atomic force microscope (AFM), magnetic tweezers, culture force monitor (CFM), and so on [7–13]. These methods are used to characterize single ligand-receptor systems through their energy landscape and kinetic parameters. Micropipette techniques [14, 15] were used to test adhesion of reconstituted model systems such as giant vesicles [16]; together with

Biomedical Optics EXPRESS

microplates, they were used to study the mechanical and adhesive properties of single cells on substrates [17] or to study cell-cell adhesion at single-cell and single-molecular levels [18]. However, these methods are not compatible with either repulsive force measurement or cell patterning at the single-cell level.

Optical tweezers, a widely utilized non-invasive tool for particle manipulation in biological applications, is a promising candidate for arbitrarily and precisely patterning cells. Because optical tweezers feature small trapping forces with high resolution, they are also a useful instrument to characterize force and to probe the viscoelastic properties of cells [19, 20], nanoparticles and DNA strands [21]. However, conventional optical tweezers require high-intensity laser beams to generate sufficient optical trapping forces, and resultant photodamage to cells limits measurement duration and its application [22]. To address this shortcoming, methods have been developed to minimize photothermal damage and increase trapping efficiency [23–26]. Specifically, we have achieved high trapping efficiency studies with a photonic-crystal platform using NIH-3T3 mammalian fibroblast, yeast and *E. coli* cells [27]. This technology inherits the versatility from conventional optical tweezers and improves trapping-force efficiency on the photonic-crystal substrate without compromising cell viability.

Human pluripotent stem cells (hPSCs) are specialized epithelial cells of the early embryo, which can differentiate into any cell type in the body. hPSCs include both embryonic stem (ES) cells derived from embryos, and induced pluripotent stem (iPS) cells derived from adult cells that have been reprogrammed into an ES cell like-state [28, 29]. hPSCs are of great interest owing to their potential for regenerative cell therapeutics and models of human biology. The ability to position hPSCs with optical tweezers could be a powerful technique for understanding and controlling such cells and their differentiated descendants. However, successful culture of hPSCs currently requires adhesive surfaces that conflict with the implementation of traditional optical tweezers. In this work, we propose and demonstrate a photonic-crystal optical tweezers system for the study of cellular interaction forces and for patterned colony formation of hPSCs.

2. Methods

We introduce a technique that allows direct manipulation of hPSCs in their culture media (mTeSR1), thereby enabling characterization of cellular interactions and colony formation through customized patterns at the single-cell level. We apply biocompatible, oxygen-plasma treated parylene-C to the tissue culture surface while simultaneously enabling manipulation of hPSCs with photonic-crystal-enhanced optical tweezers, as shown in Fig. 1. The perpendicularly incident laser on the photonic crystal in Fig. 1a generates an enhanced optical trap above the substrate and reduces photodamage to cells [27]. The photonic-crystal substrate is placed on a thermoelectric heater that can be used to adjust the temperature.

Parylene-C, which is traditionally used to coat implantable devices, has emerged as a promising material in the fabrication of miniaturized devices due to its unique mechanical properties and inertness. Although parylene-C coated on the photonic crystal is initially hydrophobic, oxygen plasma treatment of the film provides hydrophilicity and a higher degree of nanoscale surface roughness that enables cell culture comparable to standard tissue culture substrates [30]. A hydrophilic surface improves cell adhesion, which requires higher laser power to manipulate cells plated on the parylene-C surface. Therefore, its surface properties can be engineered by the plasma-treatment power and adjusted to accommodate different applications for cellular-organization studies. In fact, the hydrophobic parylene-C surface without any oxygen-plasma treatment can provide a frictionless platform to study intercellular forces.

All optical manipulations can be performed under a loosely focused low-intensity laser beam through a 20x objective lens (N.A. = 0.22). Figure 1b shows a sequence of optical manipulation images of a single hPSC on a hydrophobic parylene film (see also Visualization 1

Biomedical Optics EXPRESS

in Supplementary Materials). The red arrow indicates the trapped cell, and the white arrows designate the reference cells. The trapped cell stays fixed in its position, while the other cells move with the stage/substrate first downward, then toward the left until the trapped cell arrives at the bottom-right corner of the rectangular pattern. Throughout this process, the trapped cell experiences little friction due to the hydrophobic parylene surface. Conversely, the hydrophilic parylene-C film supports cellular colonization after patterning with the disadvantage of increased adhesion during trapping, which reveals guiding principles and trade-offs for hPSC colony formation at the single-cell level. This contrasts with a recent technique that uses geometrical confinement in micro-patterned cultures to measure cellular differentiation [1], which cannot avoid randomness in the number of cells and spacing among cells in a colony and leaves uncertainty in the study of cellular signaling during differentiation. Figure 1(c) shows a positive correlation between the oxygen-plasma power and hydrophilicity, measured by observance of the contact angle for a deionized water droplet on the surface. The inset images depict water droplets on parylene-C surfaces treated with various plasma powers.

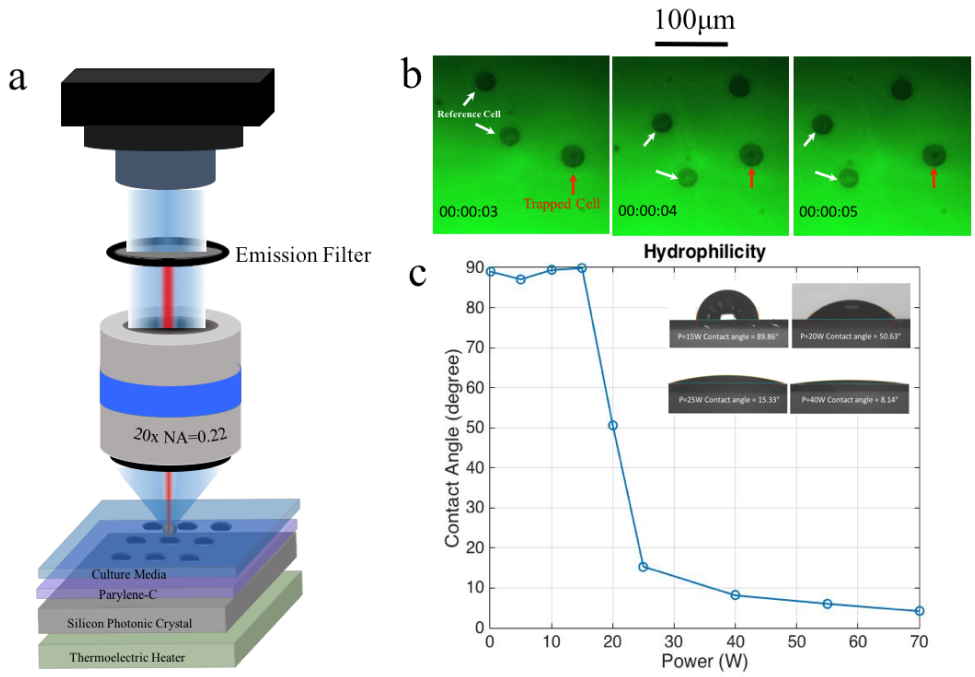

Fig. 1. Manipulation of hPSCs with a parylene-C assisted photonic-crystal optical tweezers system. (a) Schematic drawing of the photonic-crystal optical tweezers setup: a single-mode Nd:YVO_4 laser is incident on the photonic crystal perpendicularly, which improves trapping efficiency by diffraction. The parylene-C film on the substrate provides a biocompatible surface for cell culture, and the culture temperature is controlled by a thermoelectric heater seated beneath the substrate. (b) Cell movement on a hydrophobic parylene-C film using a low-intensity laser beam focused by a 20x objective lens (N.A. = 0.22). Four cells are dragged into a rectangular pattern by optical tweezers, and the movement of one cell is indicated by the relative distances between the reference cells (white arrows) and the trapped cell (red arrow), which was positioned in the corner of the rectangular pattern. (c) Relationship between plasma-treatment power and hydrophilicity of the parylene-C surface. The hydrophilicity is described by the contact angle of a deionized water droplet on the surface. The inset pictures show the droplets on parylene-C surfaces treated with different plasma powers for 30 seconds: 15 W, 20 W, 25 W, and 40 W, respectively.

Biomedical Optics EXPRESS

3. Results

3.1 Measuring intercellular force on hydrophobic parylene-C films

Cell adhesion is a fundamental property in biological systems, but is difficult to quantify using conventional microscopy [6]. To measure adhesive and anti-adhesive forces between cells, a useful approach involves manipulating single cells to measure the small forces arising between them with high resolution. To measure the intercellular forces between hPSCs, the optical trapping force was first calibrated by capturing a video of a single cell attracted to the center of a fixed laser beam with a specific intensity; Fig. 2(a) illustrates this trapping force calibration.

Cells were then plated on a hydrophobic parylene-C surface, and the laser spot was placed close to an individual cell. When the cell became attracted to the center of the laser, its position was recorded by a high-speed camera. The cell in Fig. 2(b) is tracked by a yellow box generated by the mean-shift algorithm, while the inset plot in Fig. 2(c) shows its position along the direction of motion. The blue curve in Fig. 2(c) is the derived trapping force, calculated by the velocity and acceleration parameters extracted from the video data. The theoretical trapping force, the red curve in Fig. 2(c), is computed with a computational toolbox [31] and fitted to the measured force by linear regression, yielding a determination coefficient of 0.85. Five cells were calibrated with a standard error of 5.37%.

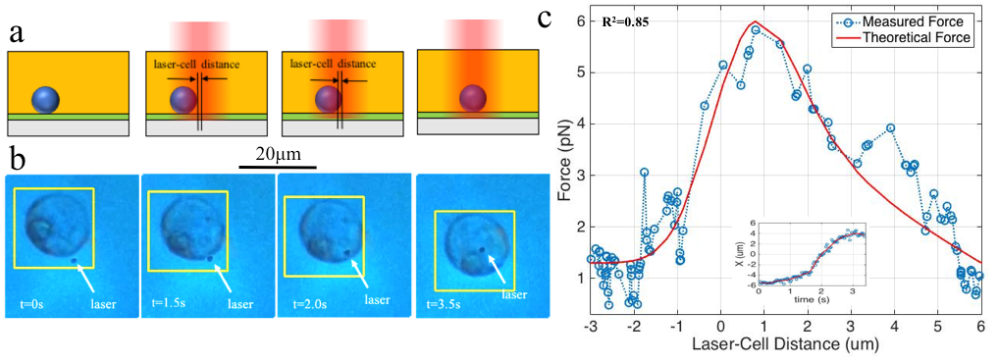

Fig. 2. Optical tweezers reveal anti-adhesive forces between hPSCs. (a) Schematic diagram of trapping force calibration: a laser beam of known intensity is placed next to a cell, which moves the cell to the center of the beam via optical gradient forces. (b) Images of an experiment showing trapping of a cell by the laser: the dark dot approximately centered in each image specifies the center of the laser beam, and cell position is tracked by a yellow box generated by the mean-shift algorithm. (c) Measured (blue) and theoretical (red) trapping forces fitted with a linear regression whose determination coefficient (R-squared value) is 0.85. The measured force is computed by Faxen's law with real-time velocity and acceleration data extracted from cell position plotted in the inset.

The procedure to measure anti-adhesive force is shown in Fig. 3(a). A pair of hPSCs expressing negatively charged podocalyxin [6] are placed near each other by the optical tweezers, and the force is then measured by centering the laser beam between the two cells. The laser trapping force pulls the cells together, while their repelling force prevents them from touching due to force balance. Therefore, a visible gap will occur in the equilibrium state. In Fig. 3(b), cells are stained with Calcein AM (CAM) dye, which emits green fluorescence due to cell metabolism, and a pair of cells are trapped as described in Fig. 3(a). The formation of a gap under optical trapping accompanied by an automatic separation after turning the laser off demonstrates the existence of a repelling force between the stem cells. A 1% HEPES buffer solution was added to the culture media during the force measurement to maintain a pH-value around 7.2–7.4. The average gap also changes over time as shown in Fig. 3(c); there are 58 data points from experiments on four different days, labeled with

Biomedical Optics EXPRESS

different colors. The average gap remains constant for the first 40 minutes of the experiments and then begins to decrease linearly. Therefore, we use the gap values measured in the first 30–40 minutes before the observed change in experimental conditions of the cell culture media.

The repulsive forces between hPSCs are characterized and shown in Fig. 3(d). A pair of cells under different laser intensities is utilized to identify the relationship between the gap and the repelling force. The separation between cells is first measured, and the repulsive forces are obtained by the calibrated trapping force discussed earlier. The blue circles in the figure are the measured gaps, and the associated forces are computed by the method described in Fig. 3(a). The red line is a linear fitting curve with an R-squared value of 0.92. Thus, the relationship between gap and force can be approximated as linear in the range of a 0.5 μm – 2 μm gap. The magnitude of the repelling force ranges from 0.3 pN – 3.6 pN, with higher forces corresponding to smaller gaps, as expected. The dotted gray lines in the plot signify trapping forces arising from different laser intensities.

The pair of cells will close the gap as the trapping force becomes higher than the repelling force. If the two cells become too close, on the other hand, the repelling force becomes greater than the trapping force and the cells separate. Therefore, the cells' equilibrium position occurs at the intersection of the repelling-force and trapping-force lines for a given laser intensity, and the intersection represents the corresponding gap. Accordingly, the second, top x-axis of the figure provides a direct correspondence between the laser intensity and the expected gap. As shown in the plot, a higher laser intensity results in a smaller gap due to a greater trapping force, which is balanced by a stronger repulsive force in the equilibrium condition. For example, the expected gap under a $0.67\ \mathrm{mW/\mu m^2}$ trapping-laser intensity is $1.15\ \mu\mathrm{m}$. The variance of the force measurement is mainly attributed to cell asynchronization during culturing, which renders cells in different phases of their cell cycle. Therefore, the repelling forces and gaps vary among different pairs of cells as shown in Fig. 3(e), even though they are members of the same cell line and experiencing the same laser intensity. In this characterization of cell interaction distribution, the gaps and repelling forces were measured under $0.67\ \mathrm{mW/\mu m^2}$ laser intensity, and the peak of the gap distribution was at $\sim 1.05\ \mu\mathrm{m}$, which matches the linear regression result in Fig. 3(d). Visualization 2 in Supplementary Materials shows the visualization of one trapped hPSC pushing the other through the repelling force. A gap between the cells can be clearly seen. Visualization 3 shows two cells held closely together by the trapping laser, and they later repel one another after the laser is turned off.

Biomedical Optics EXPRESS

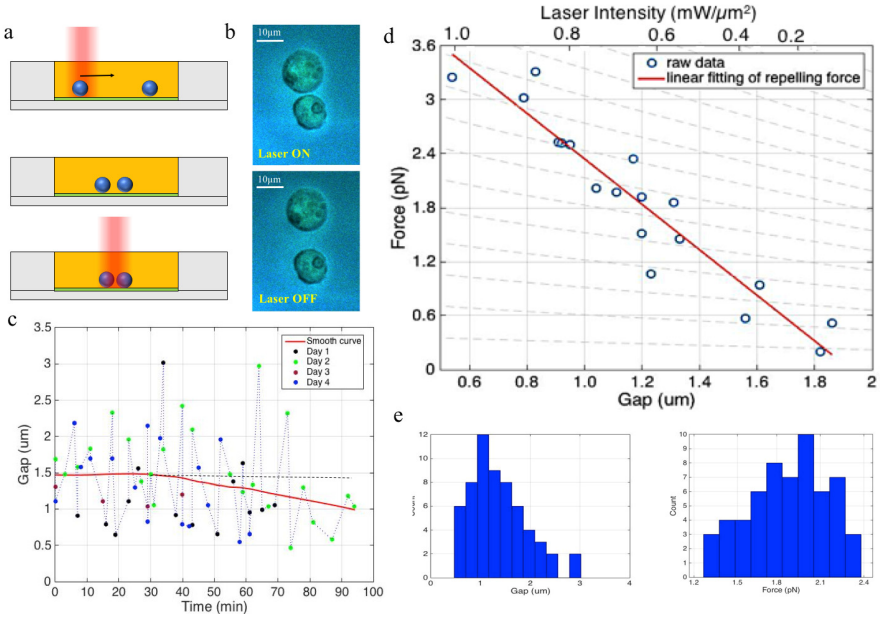

Fig. 3. (a) Schematic drawing of the repulsive force measurement where two cells were positioned close to each other, and the laser beam was placed in the middle of the two cells. (b) The gap between cells with or without laser-induced forces. A pair of CAM-stained cells remain separated by a gap when the laser is turned on at the center position between them. When the laser is off, the cells repel each other becoming further separated. (c) Average gap change over time with a laser intensity of 0.67 mW / μm^2. The time indicates the start of the experiments each day, and the gaps were measured over time. The red line describes a moving average filter, and the black dotted line is an extension representing the average value of the gap before decreasing. The average gap stays the same during the first 40 minutes and decreases afterwards, which indicates the valid period of measurement. (d) Repulsive force characterizations. The repulsive force decreases with a wider gap, given a set laser intensity. (e) Histograms of gaps and corresponding repulsive forces. The gaps were measured for multiple pairs of cells in a single experiment on a single day. The histograms show the resulting distribution of intercellular forces among these pairs of cells.

3.2 Cellular spatial patterning on oxygen-plasma-treated parylene-C films

The hydrophilic parylene-C surface after proper oxygen-plasma treatment can support both cell manipulation and colony formation. Figure 4(a) illustrates the procedure for patterning cells using photonic-crystal optical tweezers followed by cell culturing. The photonic-crystal silicon substrate was coated with a 2 μm -thick parylene-C film that underwent oxygen-plasma treatment for 30 seconds. Cells on the substrate were patterned via optical manipulation, and Geltrex (Fisher Scientific) was then mixed into the culture media. Geltrex is an extracellular matrix that is necessary for adherent culture of hPSCs. After heating to 37 °C, cells began to spread out and attach to the surface. Higher hydrophilicity improves cell adhesion and requires higher laser intensity that can cause severe photo-damage to the cells, whereas a hydrophobic surface cannot support cell attachment and growth. Therefore, proper plasma treatment and surface hydrophilicity were explored.

Cells were cultured on the parylene-C surfaces treated with different plasma powers, and Geltrex was added after plating the hPSCs. Figure 4(b) shows the cell culture results for 15 W, 20 W, 30 W, 45 W, 55 W, and 70 W of plasma power on the first and sixth days of the experiment. On the first day of cell culture, all surfaces had cells attached, but the surface that underwent a 15 W plasma treatment had no colonies on the sixth day, while the colonies on the other surfaces increased with plasma power. The colonies on the 70 W plasma-treated surface were almost confluent on the sixth day. To consider the results more quantitatively,

Biomedical Optics EXPRESS

the cultured cells were passaged with Accutase on the seventh day and counted by a CASY Cell Counter (OMNI Life Science). The average cell density on the glass chips could then be calculated, as shown in Fig. 4(b). In general, the average cell density on the parylene films increases with higher plasma power due to better surface biocompatibility for cell culture. Therefore, higher oxygen-plasma power during treatment provides a better surface to which cells can adhere and form colonies, and 20 W was determined as the minimum threshold required to culture hPSCs. However, as mentioned, higher plasma powers require higher laser intensities to manipulate cells. Optimally, to reduce the photodamage to cells during manipulation while simultaneously producing a culture surface, we utilized a 20 W oxygen-plasma treated parylene-C film in subsequent experiments.

Figure 4(c) shows two cell-patterning results generated with more than eight cells using the photonic-crystal optical tweezers. A 20 W oxygen-plasma-treated parylene film allows sufficient time to form stable cell patterns while at the same time allowing manipulation of the cells with weak optical forces. Compared with cell manipulation results on conventional tissue culture surfaces [32], the treated parylene-C film on the photonic crystals allows construction of patterns with more cells. To demonstrate, in Fig. 4(c), an "R" pattern on the left and a rotated "π" pattern on the right consisting of eight and ten cells were achieved on photonic-crystal substrates, respectively. All of these cells adhered to the surface after adding Geltrex at 37 °C. As shown in Fig. 4(d), cells were initially patterned into the shape of a key on the photonic crystal, and after 35 minutes of incubation at 37 °C, some cells began to spread out on the parylene-C film, which indicated cell attachment to the surface. Firm cell-surface attachment allows movement of the Petri dish to an incubator without destroying the patterns before continuing cell culture. During the 35 minutes of incubation, cells may also migrate to other locations before spreading out. For example, in the right image of Fig. 4(d), the cell serving as the tooth of the key does not spread out until moving off the photonic crystal region.

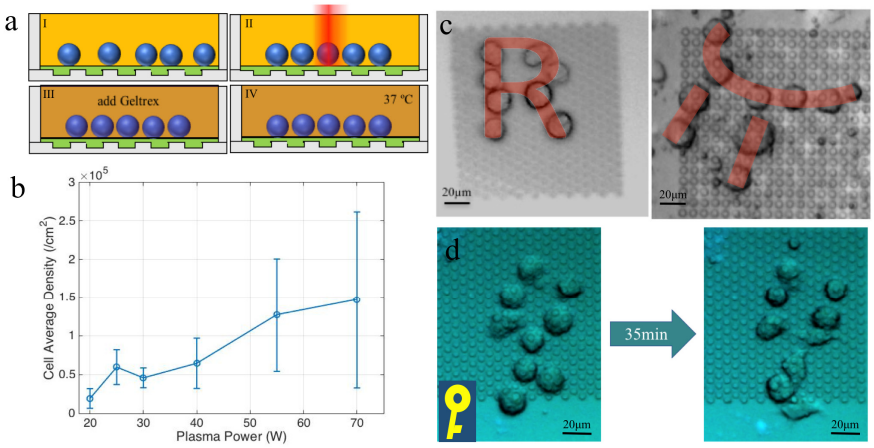

Fig. 4. Cellular spatial patterning at the single-cell level. (a) Schematic drawing of the patterning process. Randomly plated cells were first patterned by photonic-crystal optical tweezers before adding Geltrex to the solution. Cells began to attach to the parylene-C film after heating up to 37 °C. (b) Cell average density on glass slides coated with various oxygen-plasma treated parylene-C films. (c) Cellular patterning using photonic-crystal optical tweezers. The photonic crystal substrate was coated with a parylene-C film that underwent 20 W of plasma treatment. An "R" pattern (left) and "π" pattern (right) were constructed on the photonic-crystal platforms. (d) A key shaped pattern of stem cells on a photonic crystal coated with parylene-C after a 20 W plasma treatment. The left bottom corner shows a schematic picture of the key pattern. Cells began to spread out and attach to the surface after 35 minutes of heating at 37 °C. The cell that is the tooth of the key does not attach until migrating to the key's bottom.

Biomedical Optics EXPRESS

4. Conclusion

In this work, we demonstrate a novel optical tweezers method for characterizing interaction forces and successfully forming colonies of arbitrarily patterned hPSCs. This approach utilizes optical-beam modulation through photonic crystals integrated with parylene-C films that provide the optimal tissue culture surface for various cell manipulation applications. We experimentally verified and characterized an anti-adhesive intercellular force between single hPSCs on the hydrophobic parylene-C surface. This method has been applied to studying podocalyxin as a possible mechanism for anti-adhesion behavior among hPSCs, which is critical in proper junctional organization in kidneys [6]. We also demonstrated that this method can enable culturing of patterned hPSCs after optical manipulation by using parylene-C surfaces treated with the appropriate oxygen-plasma power. This optimal power was explored, and the method achieved both cell culturing and cell manipulation with low laser intensity.

Funding

National Science Foundation (NSF) IDBR program (DBI-1353718); National Institutes of Health Award (DK102826, NIDDK, to BSF).

Acknowledgments

The photonic crystals, coated with parylene-C films, were fabricated in the Washington Nanofabrication Facility (WNF), and oxygen-plasma treatment occurred in the Photonics Research Center, Department of Chemistry at the University of Washington. We thank Professor Suzie Pun's group in UW Bioengineering for assistance through usage of her cell culturing facilities, and Assistant Professor Hongxia Fu (UW Hematology) for helpful discussions.

Disclosures

The authors declare that there are no conflicts of interest related to this article.